CFD STUDY OF STEAM CONDENSING FLOW IN A LAVAL NOZZLE

Rodrigo Dias Vilela, vilela@ita.br
Cláudia Regina de Andrade, claudia@ita.br
Edson Luiz Zaparoli, zaparoli@ita.br
Instituto Tecnológico de Aeronáutica, Departamento de Engenharia Aeronáutica e Mecânica, Área de Aerodinâmica, Propulsão e Energia – Praça Marechal Eduardo Gomes, 50, Vila das Acácias, CEP 12.228-900, São José dos Campos, SP, Brasil.

Aluisio Viais Pantaleão, aluisio.pantaleao@vsesa.com.br
Vale Soluções em Energia S.A.– Rodovia Presidente Dutra, s/n, km 138, Eugênio de Melo, CEP 12.247-004, São José dos Campos, SP, Brasil.

Abstract. *The process of condensing steam inside turbines damage their internal surfaces and also reduces the aerodynamic efficiency in that region. As a frame for study of the condensation in turbine stages, it is proposed in this paper a simpler case, having the wet steam flow set in a 2D transonic Laval nozzle (convergent-divergent). This geometry is selected due to possibility to validate the CFD code on the basis of experimental data for Laval nozzles. The goal is to investigate how the variation of the thermal parameters, such as temperature and pressure, changes the condensation onset by examining the region of nucleation and growth of steam droplets along the flow direction. The condensation phenomena is modeled on the basis of the classical nucleation theory. In this work, the mathematical model of this multiphase compressible flow is numerically solved using finite volume method with a coupled density-based approach. Turbulence models were used in the numerical simulations as comparation with the experimental available data. The simulation results shows that for avoiding condensation inside the nozzle must consider the possibility of elevating the temperature of steam at the entrance or decreasing the pressure difference established between the input and output.*

Keywords*: wet steam flow, condensation, Laval nozzle, multiphase, CFD modeling*

1. INTRODUCTION

For several decades, theoretical and experimental study on the design of steam turbines was been highly investigated. The need to solve problems in the construction of turbines is increasing in industrial and technological development, seeking to improve the process of power generation. In this ongoing effort to achieve greater efficiency as well as durability, the numerical approach appears as a new search technology aimed at a more advanced manufacturing.

The condensation process takes place during the steam flow through the low-pressure (LP) turbine. During the operation of a steam turbine, the superheated steam getting into the it, transferring thermal energy to the movement of the blades, seeping through some stages, comes in the form of satured steam, showing a small fraction of liquid at low-pressure turbine (these also are known as wet steam turbines, for operating the steam saturation line). This fraction varies according to turbines design. That thin layer of liquid water can cause erosion on the inner surface of the turbine blades.

Wróblewski et al. (2009) presented a numerical method for modeling transonic steam flows with homogeneous and/or heterogeneous condensation. The experiments carried out for the Laval nozzles, for 2D turbine cascades and for a 3D flow in real turbine were selected to validate an in-house CFD code adjusted to the calculations of the steam condensing flows in complicated geometries. The main intention was not to show the best results of possible solutions, but to pay attention to the big sensitivity of the condensation models to the flow conditions (e.g. inlet parameters, steam quality) and implemented gas equation of state. The validation has been performed for many test cases, including flow through the 3D steam turbine stages as well with generally good degree of accuracy.

Kermani and Gerber (2003) performed numerical evaluations of thermodynamic and aerodynamic losses in nucleating steam flow in a series of converging/diverging nozzles with and without shocks. The model showed that the overall thermodynamic loss is only mildly influenced by increasing shock strength, while the aerodynamic losses follow that of the single phase flow, and are of the same magnitude as the thermodynamic loss only in the case of very weak shocks. The thermodynamic losses can be attributed to two influences, the homogeneous nucleation event, and the post-shock thermal oscillations in the two-phase system.

Moses and Stein (1978) performed experimental investigations on the growth of steam droplets formed in a Laval nozzle using both static pressure and light scattering measurements. A series of experiments on steam condensation have been made in a Laval nozzle over a variety of starting conditions such that the onset of condensation occurs in the range 233 to 313 K. They have concluded that the majority of the condensed phase is due to droplet growth. For detailed calculations on one of the experiments there was excellent agreement with both measurements throughout the condensation zone and theoretical calculations using the classical nucleation rate expression and droplet growth laws.

At the present work, a numerical study is performed on steam condensing flow in a 2D Laval nozzle. Numerical results are compared with experimental ones provided by Moses and Stein (1978). The governing equations (mass, energy and momentum conservation) were solved using a commercial code with the wet steam model coupled with two-equations turbulence model (realizable $k-\varepsilon$ and SST $k-\omega$), in order to investigate the condensation phenomena, analyzing different thermal parameters in Laval nozzle.

2. MATHEMATICAL FORMULATION

2.1. Governing equations and assumptions

The mixture flow is governed by the compressible Navier-Stokes equations in conjunction with a wet steam multiphase model. To solve the problem a CFD code (FLUENT package), that adopted the Eulerian-Eulerian approach for modeling wet steam flow, was used. The governing equations (mass conservation, momentum, energy and turbulence model) are stated as:

$$\frac{\partial \rho}{\partial t} + \frac{\partial}{\partial x_i}(\rho u_i) = S_m \tag{1}$$

$$\frac{\partial}{\partial t}(\rho u_i) + \frac{\partial}{\partial x_j}\left(\rho u_i u_j\right) = -\frac{\partial P}{\partial x_i} + \frac{\partial \tau_{ij}}{\partial x_j} + \mathrm{S}_{u_i} + \mathrm{S}_{\mathrm{F}_i} \tag{2}$$

$$\frac{\partial}{\partial t}(\rho H) + \frac{\partial}{\partial x_j}\left(\rho u_j H\right) = \frac{\partial P}{\partial t} + \frac{\partial}{\partial x_j}\left[\Gamma_E \frac{\partial T}{\partial x_j}\right] + S_w + S_d + S_h \tag{3}$$

where x_i are the Cartesian coordinates; u_i are the corresponding average velocity components; t is the time; ρ is mixture density; P is pressure; τ_{ij} are stress tensor components; T is average temperature; H is total enthalpy; Γ_E is effective thermal conductivity. The term S_m is the mass source (defined to reflect the condensation and vaporization process); S_{u_i} contain source representing momentum exchange between the water droplets and surrounding gas; $\mathrm{S}_{\mathrm{F}_i}$ contains the smaller terms from gradient of the Reynolds stress tensor; $S_w + S_d$ represents the total viscous stress energy contribution; and S_h contains the interphase heat transfer.

- Equations of the Realizable $k-\varepsilon$ turbulence model:

$$\frac{\partial}{\partial t}(\rho k) + \frac{\partial}{\partial x_j}\left(\rho k u_j\right) = \frac{\partial}{\partial x_j}\left[\left(\mu + \frac{\mu_t}{\sigma_k}\right)\frac{\partial k}{\partial x_j}\right] + G_k - \rho\epsilon - Y_M \tag{4}$$

$$\frac{\partial}{\partial t}(\rho \epsilon) + \frac{\partial}{\partial x_j}\left(\rho \epsilon u_j\right) = \frac{\partial}{\partial x_j}\left[\left(\mu + \frac{\mu_t}{\sigma_\epsilon}\right)\frac{\partial \epsilon}{\partial x_j}\right] - \rho C_2 \frac{\epsilon^2}{k + \sqrt{\upsilon\epsilon}} \tag{5}$$

where $k =$ turbulenct kinetic energy; $\epsilon =$ turbulent energy dissipation rate; $\mu =$ molecular viscosity; $\mu_t =$ turbulent viscosity; G_k represents the generation of turbulence kinetic energy due to the mean velocity gradients; Y_M represents the contribution of the fluctuating dilatation in compressible turbulence to the overall dissipation rate; C_2 are constants; υ is kinematic viscosity; σ_k and σ_ϵ are the turbulent Prandtl numbers for k and ϵ, respectively. The constant values of the Realizable $k-\varepsilon$ model used in this work are: $\sigma_k = 1.0$; $\sigma_\epsilon = 1.2$; $C_2 = 1.9$.

- Equations of the SST $k-\omega$ turbulence model:

$$\frac{\partial}{\partial t}(\rho k) + \frac{\partial}{\partial x_i}(\rho k u_i) = \frac{\partial}{\partial x_j}\left(\Gamma_k \frac{\partial k}{\partial x_j}\right) + \tilde{G}_k - Y_k \tag{6}$$

$$\frac{\partial}{\partial t}(\rho \omega) + \frac{\partial}{\partial x_i}(\rho \omega u_i) = \frac{\partial}{\partial x_j}\left(\Gamma_\omega \frac{\partial k}{\partial x_j}\right) + G_\omega - Y_\omega \tag{7}$$

where $\omega =$ turbulent energy dissipation rate; $\tilde{G}_k$ represents the generation of turbulence kinetic energy due to mean velocity gradients; G_ω represents the generation of ω; Γ_k and Γ_ω represent the effective diffusivity of k and ω, respectively; Y_k and Y_ω represent the dissipation of k and ω due to turbulence. The constant values of the SST

k − ω model used in this work are: $\sigma_{k,1} = 1.176$; $\sigma_{k,2} = 1.0$; $\sigma_{\omega,1} = 2.0$; $\sigma_{\omega,2} = 1.168$; $\beta_{i,1} = 0.075$; $\beta_{i,2} = 0.0828$; $\beta_{\infty}^{*} = 0.09$.

The following assumptions are made in the wet steam model: the volume occupied by droplets is negligibly small and the mass fraction of the condensed phase, β (also known as wetness factor), is small ($\beta < 0.2$); the interaction between the droplets are neglected; the heat exchange between the liquid phase and the solid boundary as well as the velocity slip between the droplets and gaseous-phase is not taken into account in the model.

In this model, two additional transport equations are required. The first transport equation governs the mass fraction of the condensed liquid phase (β):

$$\frac{\partial \rho\beta}{\partial t} + \frac{\partial}{\partial x_i}(\rho u_i \beta) = \Gamma \tag{8}$$

where Γ is the mass generation rate due to condensation and evaporation (kg per unit volume per second). The second transport equation models the evolution of the number density of the droplets per unit volume (η):

$$\frac{\partial \rho\eta}{\partial t} + \frac{\partial}{\partial x_i}(\rho u_i \eta) = \rho I \tag{9}$$

where I is the nucleation rate (number of new droplets per unit volume per second).

The mass generation rate Γ in the classical nucleation theory during the non-equilibrium condensation process is given by the sum of mass increase due to nucleation (the formation of critically sized droplets) and also due to growth/demise of these droplets. Therefore, Γ is written as:

$$\Gamma = \frac{4}{3}\pi\rho_l I {r_*}^3 + 4\pi\rho_l \eta \bar{r}^{\,2}\frac{\partial \bar{r}}{\partial t} \tag{10}$$

where ρ_l is the liquid density, $\bar{r}$ is the average radius of the droplet, and r_* is the Kelvin-Helmholtz critical droplet radius, above which the droplet will grow and below which the droplet will evaporate.

The nucleation rate I described by the steady-state classical homogeneous nucleation theory and corrected for non-isothermal effects is given by:

$$I = \frac{q_c}{(1+\theta)}\left(\frac{\rho_v^2}{\rho_l}\right)\sqrt{\frac{2\sigma}{{M_m}^3\pi}}\, e^{-\left(\frac{4\pi {r_*}^2 \sigma}{3k_b T}\right)} \tag{11}$$

where q_c is evaporation coefficient, k_b is the Boltzmann constant, M_m is mass of one molecule, σ is the liquid surface tension, and ρ_v is the vapor density at temperature T.

2.2. Boundary conditions

The geometry of the nozzle was reproduced with Gambit 2.4.6 software, as a detailed description of Moses and Stein (1978), but only half computational domain was sufficient to represent the nozzle due to its symmetry, as shown in Fig. 1. The mesh was constructed in order to follow the flow, facilitating the solution convergence. The boundary conditions are also presented in Fig. 1, where the total pressure P_0 and total temperature T_0 are prescribed in the inlet; static pressure P and total temperature are prescribed in the outlet.

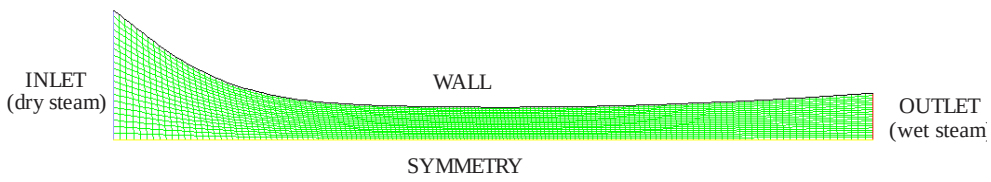

Figure 1. Geometry, mesh and boundary conditions

3. VALIDATION PROCEDURE

To validate the numerical procedure, the test case considered a transonic wet steam flow under the conditions corresponding to the experiment number 410 provided by Moses and Stein (1978) experimental work. The precise preparation of the steam used for experiment assured, according to author's explanations, the pure homogeneous

character of the observed condensation process. In their experiment (Exp. 410), it was considered with no initial moisture entering the nozzle (superheated vapor), when the dry steam is supplied to the nozzle inlet and hence the droplets are forming due to only spontaneous condensation. Calculations were performed for nozzle with inlet stagnation conditions $P_0 = 70727.32$ Pa and $T_0 = 377$ K; and in outlet, $P = 5000$ Pa and $T = 377$ K. The numerical results are compared with the experimental data in Fig. 2.

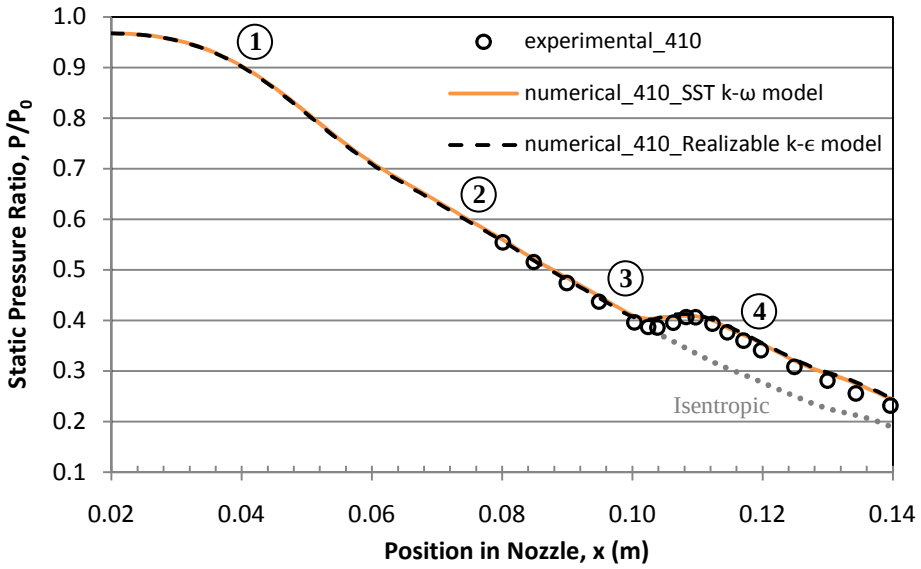

Figure 2. Centerline pressure distributions compared to the results of Moses and Stein (1978)

As shown at Fig.2, the predicted centerline pressure profile is very good for the condensation shock location in both turbulence models. Therefore, the agreement with experiment is observed. The process can be analyzed in the following steps:

1. The steam expands isentropically into the converging portion of the nozzle;

2. It crosses the vapor-liquid equilibrium line where the saturation ratio $S = (P/P_\infty)T = 1$, i. e. the steam is saturated vapor (P_∞ is the liquid-vapor equilibrium pressure at the temperature T). The point 2 may occur in the converging (subsonic) part of the nozzle or in the diverging (supersonic) section, depending on the conditions P_0 and T_0. Since the expansion cools the flow at a very high rate, condensation does not appear in this point;

3. When the pressure becomes greater than the local vapor pressure (supersaturation), the nucleation rate increases rapidly and a very large number of stable molecular clusters are formed, releasing the heat of vaporization to the flow deviates the thermodynamic isentropic behavior. The point at which the pressure differs from the isentropic value by 1 percent is commonly called the "onset of condensation";

4. The length along the nozzle between points 3 and 4 is known as the "condensation zone". At the end of condensation zone, the thermodynamic state of the vapor is near the equilibrium line. The process for droplet growth slows down and the flow again begins to expand and cool.

4. RESULTS

For the simulations was used the geometrical according to the Fig. 1, where a detailed study of mesh refinement was conducted to ensure the confiability of the results. In the validation process was shown that both turbulence models reproduce a good agreement with experimental data, but only the SST $k-\omega$ model was used in the subsequent simulations because information available in the literature report that this is the most appropriate model for problems similar to those presented in this paper.

The convergence criterion in all cases was the residue of the mass balance of less than 10^{-6}, as well as the constant velocity profile of an interaction to another.

4.1. Influence of Turbulence Intensity

The wet steam model equations contains no dependent parameter of the turbulence, but is important to investigate if any change in the level of turbulence will cause variations in the flow and therefore, in the amount of condensed mass. In that case, the thermal parameters were kept constant with inlet stagnation conditions $P_0 = 70$ kPa and $T_0 = 378.16$ K; and in outlet, $P = 5$ kPa and $T = 378.16$ K. Condensation inside the nozzle is shown in Fig. 3.

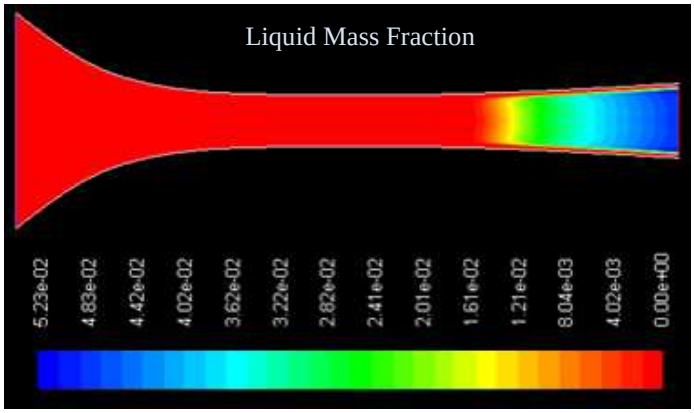

Figure 3. View of the effect of turbulence on spontaneous condensation.

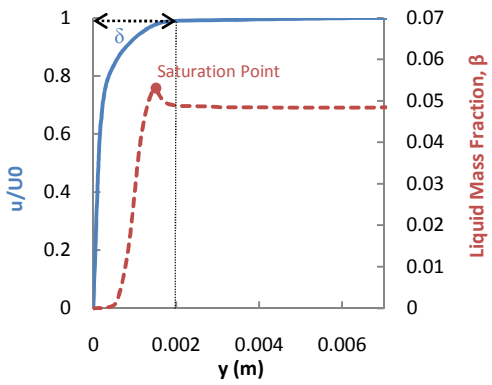

Figure 4. Velocity profile and condensed fraction along the y-axis at the nozzle exit.

Figure 3 shows a region near the wall where no condensation occurs. That fact happens because the boundary condition on the wall establishes a non-slip condition, therefore, the velocity of the steam decreases within the turbulence boundary layer (Fig. 4) and, thus, the temperature increases across the saturation point, returning to the state of superheated vapor in this region. At such location, the calculated turbulent boundary layer thickness, δ, was 1.99 mm.

The average amount of liquid mass in the nozzle exit was calculated for some values of turbulence intensity in a 2 to 25% range; shown in Fig. 5.

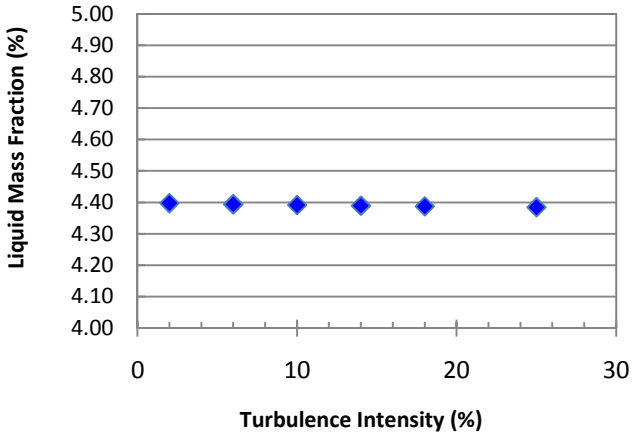

Figure 5. Variation of liquid mass fraction for different turbulence intensities.

It is noted that the fraction of liquid mass remains approximately constant, indicating that this parameter does not influence the amount of condensed water to the nozzle, indicating that such parameter only affects the pattern of flow. For that reason, all subsequent simulations were performed with the value of turbulence intensity equals to 10%.

4.2. Influence of Temperature

The temperature is an important parameter in the condensation of steam. To illustrate its influence, the phenomenon of supersaturation in the nozzle must be understood, considering the scheme shown in Fig. 6. The dry steam follows the path 1-*a* on a T-*s* diagram, where the steam should condense at point *a*. However, as the point *a* is located in the divergent nozzle part, condensation does not occur until the point *b* is reached. At that point, the condensation occurs abruptly and is called "condensation shock". Between the points *a* and *b* water occurs as steam, but the temperature is lower than the saturation temperature for the given pressure. Thus, steam is a metastable

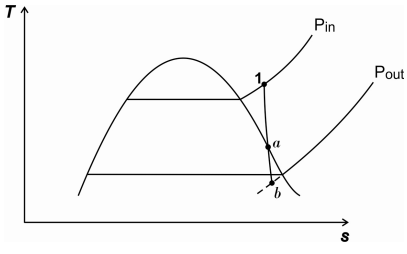

Figure 6. Scheme of supersaturation.

state between *a* and *b*. This means that droplets smaller than a critical size evaporate again and only droplets larger than this critical size are formed, generating a new state of equilibrium. The small variation in the entropy is due to the condensation shock.

To investigate how the fraction of liquid mass depends on temperature, the stagnation pressure at the entrance and the exit static pressure were kept constant, $P_0 = 70$ kPa and $P = 5$ kPa, respectively, only the steam temperature at the entrance was varied. The results are shown in Fig. 7.

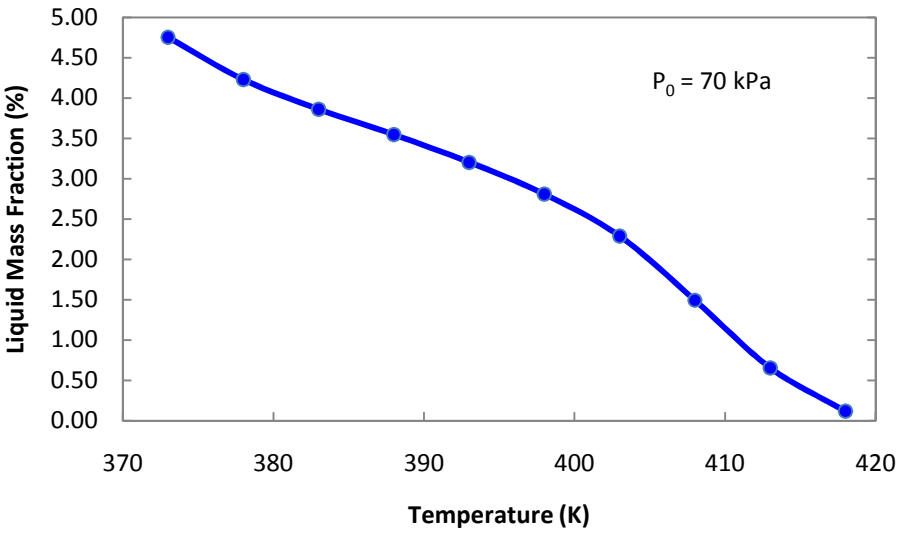

Figure 7. Variation of liquid mass fraction for different temperatures.

The first point (T = 373 K) in Fig. 7 represents the temperature as closer to saturation as possible to simulate. This difficulty in simulating a flow in which the steam enters the nozzle in a state close to saturation is due to the limitation of the wet steam model, which assumes that the wetness factor is small. Note that as the steam temperature increases, the average liquid mass fraction in the nozzle exit decreases to the point where no condensation occurs inside the nozzle (T = 418 K, approximately). Raising the temperature above that value, the steam will not cross the saturation line and it will leave the nozzle in the form of dry steam.

4.3. Influence of Pressure

The pressure is perhaps the most important parameter in the design of steam turbines. For this reason it was analyzed its influence on the process of condensation of steam inside the nozzle.

In that case, the temperature remained constant $T_0 = 378.16$ K while the pressure difference, ΔP, was varied. The phenomena of nucleation and condensation are shown in Fig. 8. The steam expands to cross the line of saturation and then the nucleation of droplets starts to increase rapidly to a peak, where the growth of the steam droplets increases its volume and hence, the amount of condensed mass.

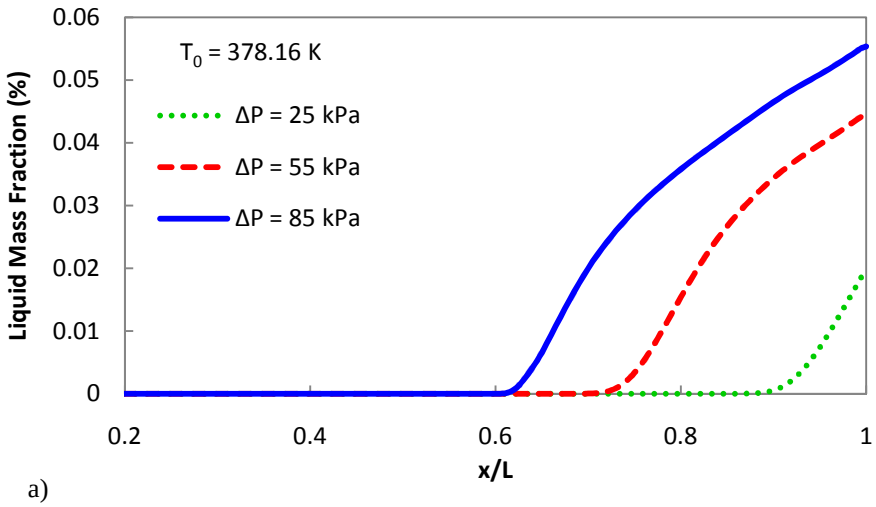

a)

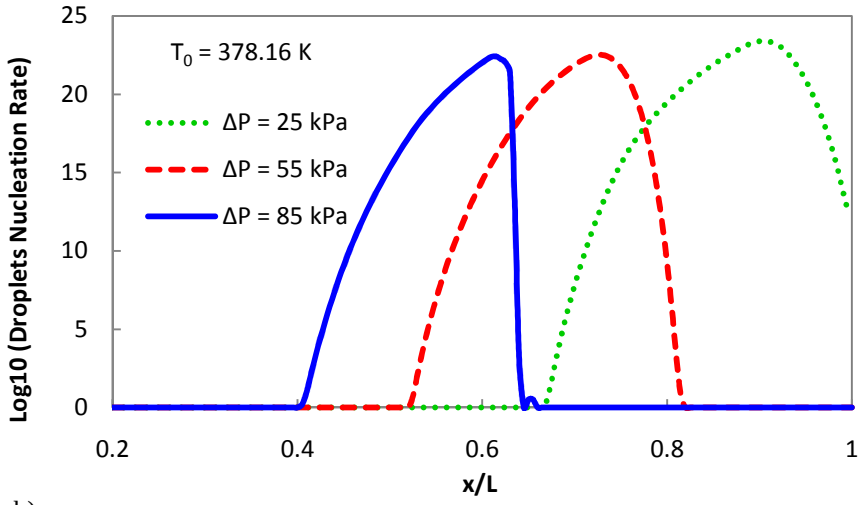

b)

Figure 8. a) Condensed phase and b) Nucleation in centerline as a function of position in the nozzle (L is the total length in the x-axis).

Figure 8 shows the dynamics of condensation for three pressure differences. Observe that there is an anticipation of condensation with increasing pressure difference, and that happens because, with increasing inlet pressure, the steam gets near the saturated state, facilitating the condensation. When the pressure difference is reduced, a delay in condensation occurs, with a minimum point (ΔP = 15 kPa, approximately) necessary for the steam to cross the saturation line inside the nozzle. Further decreasing the pressure difference, no condensation occurs.

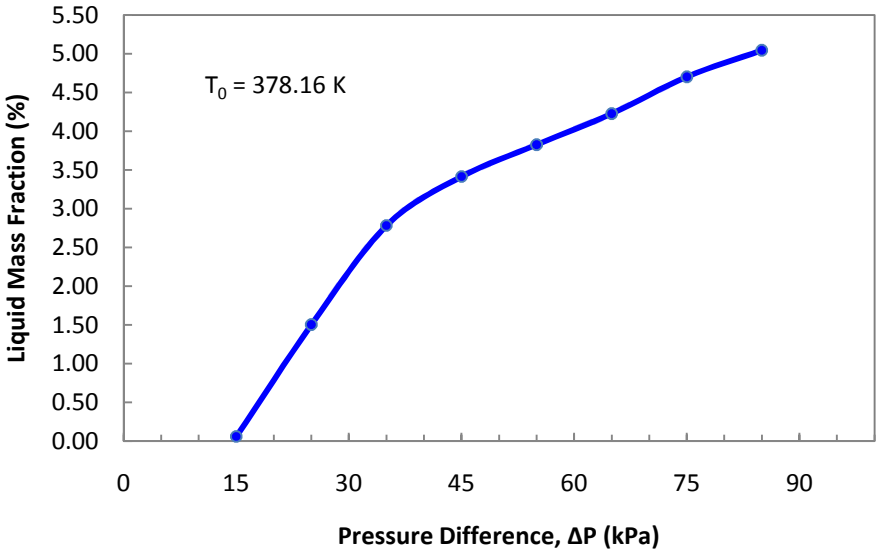

Figure 9. Variation of liquid mass fraction for different pressure differences.

The minimum point can be seen in Fig. 9, which shows the average liquid mass fraction in the exit in relation to the pressure difference, established between input and output nozzle.

Unlike the temperature, the liquid mass fraction increases with increasing pressure difference to the point where the steam is already in the form of saturated steam, but that item is not presented due to the limitation of the model (not converge for high values of β).

5. CONCLUSIONS

In this work a numerical study was performed in order to analyze the steam condensing flow in a Laval nozzle. Numerical simulations have been described and used to investigate the influence of the thermal parameters on changes of the condensation onset by examining the region of nucleation and growth of steam droplets along the flow direction.

Before varying the conditions of entry of steam, an analysis of the influence of turbulence intensity on the condensate was made, representing a region of no condensation inside the turbulent boundary layer, but the variation of liquid mass fraction at the outlet was negligible. Then, the temperature and pressure at the entrance of the nozzle were varied and showed that the onset of condensation zone moves along the nozzle and; therefore, varies the average liquid mass fraction in the nozzle exit. Figure 7 shows that by raising the temperature of steam at the entrance, the point of condensation is delayed, presenting a maximum limit to the phenomenon that occurs inside the nozzle. An opposite behavior occurs for the pressure, shown in Figure 9, since this delay is due to the decrease of pressure difference established between the input and output, with a minimum value for condensation to occur in the nozzle.

Therefore, a project of the steam turbine, which wishes to avoid condensation inside it, must consider the possibility of elevating the temperature of steam at the entrance or decrease the pressure difference established between the input and output. This is desirable, but other difficulties in the project may appear due to these considerations.

6. REFERENCES

Bakhtar, F., Ebrahimi, M., Webb, R.A., 1995. On the performance of a cascade of turbine rotor tip section blading in nucleating steam – Part 1: surface pressure distributions. In: Proceedings of the Institution of Mechanical Engineers Conference Publications, Part C – Journal of Mechanical Engineering Science, vol. 209, pp. 115–124.

Bakhtar, F., Ebrahimi, M., Bamokle, B.O., 1995. On the performance of a cascade of turbine rotor tip section blading in nucleating steam – Part 2: wake traverses. In: Proceedings of the Institution of Mechanical Engineers Conference Publications, Part C – Journal of Mechanical Engineering Science, vol. 209, pp. 169–177.

Barschdorff, D., 1971. Verlauf der Zustandsgrossen und gasdynamische Zusammenhaenge der spontanen Kondensation reinen Wasserdampfes in Lavalduesen. Forsch. Ingenieurwes. 37, 146–157.

Gyarmathy, G., 2005. Nucleation of steam in high-pressure nozzle experiments. In: Proceedings of 6th European Conference on Turbomachinery, Lille, France, pp. 458–469.

Hill, P.G., Condensation of water vapor during supersonic expansion in nozzles, J. Fluid Mech. 25 (1966) 593–620 (Part 3).

Kolovratnik, M., 2006. Measurement of concentration and size of droplets in the steam flow at exit of the low pressure part of the 360MW turbine in the Bełchatow Electric Power Plant, Czech Technical University in Prague, Faculty of Mechanical Engineering, Technical Report, Prague, November.

Moses, C.A., Stein, G.D., 1978. On the growth of steam droplets formed in a Laval nozzle using both static pressure and light scattering measurements. J. Fluids Eng. 100, 311–322.

Nikkhahi, B., Shams, M., Ziabasharhagh, M., A numerical investigation of two-phase steam flow around a 2-D turbine's rotor tip. International Communications in Heat and Mass Transfer 36 (2009) 632–639

White, A.J., Young, J.B., Walters, P.T., 1996. Experimental validation of condensing flow theory for a stationary cascade of steam turbine blade. Philos. Trans. Roy. Soc. Lond. A 354, 59–88.

Wroblewski, W., Dykas*,S., Gepert, A., Steam condensing flow modeling in turbine channels. International Journal of Multiphase Flow 35 (2009) 498–506

7. RESPONSIBILITY NOTICE

The authors are the only responsible for the printed material included in this paper.